Time-Varying Linear Quadratic Gaussian Optimal Control for Three-Degree-of-Freedom Wave Energy Converters

Ossama Abdelkhalik, Shangyan Zou, Rush Robinett, Umesh Korde
Department of Mechanical Engineering
Michigan Technological University
Houghton, Michigan 49931

***Abstract*—The model of a three-degree-of-freedom Wave Energy Converter can be simplified as a linear time-varying system. In this model, the heave mode parametrically excites the pitch mode, which in turn excites the surge mode. The heave mode, however, is independent to the other two modes when the motion is small. The purpose of this paper is to design a controller to maximize the energy harvested over a receding time horizon. We also want to demonstrate that, with proper design of the control, it is possible to exploit this nonlinear coupling between the modes so as to harvest more energy. The controller selected is the linear quadratic Gaussian optimal control. The prediction of excitation forces is constructed based on the estimation where the estimations are obtained by using extended Kalman Filter. The prediction of excitation force is fed into the controller to compute the time-varying linear quadratic optimal control. Constraints on the WEC motion are accounted for in computing the control. The results show that the energy captured by three-degree-of-freedom Wave Energy Converter is 3.56 times the energy extracted in heave mode only. Higher energy harvesting is demonstrated when the linear time-varying model is used in control design.**

***Index Terms*—Wave Energy Conversion; Surge-Heave-Pitch control; Linear Quadratic Gaussian Controller; Time-varying system; Wave Prediction**

I. Introduction

Wave energy is one of the sustainable sources of energy characterized by its high density [1]. The assessment of the power density of the wave continues worldwide [2]–[5] and shows a good potential for wave energy. Assessment and experimental testing of Wave Energy Converters (WECs) also continues [6]–[13]. Nowadays, a number of different WECs have been built [14] which can extract energy from different modes of motion. Types include the overtopping devices such as WaveDragon [15], the pitching devices such as Pelamis [16] and the heaving devices such as AquaBuOY [17].

Hydrodynamics and equations of motion of wave energy converters have been studied extensively in early works [18]–[22]. Also the efficiency of one-degree-of-freedom (1-Dof) and two-degree-of-freedom (2-Dof) WECs are discussed in several references. Several relatively recent studies have focused on the control of WECs, e.g. [23]–[26], mostly for 1-Dof WECs. For example, reference [27] uses a pseudo-spectral method to reduce the complexity of the system through approximation. A Model Predictive Control (MPC) is developed in [28]. The MPC needs a wave prediction over a future horizon. A Linear Quadratic Gaussian (LQG) controller was developed in [29] for a linear time-invariant dynamics model WEC.

Early studies in wave energy conversion have pointed out the advantage of harvesting wave energy from an antisymmetric mode such as surge or pitch because the antisymmetric radiation pattern it generates, which can potentially enhance energy conversion for waves approaching from a certain direction [20]. Optimum conversion requires oscillations to maintain a certain amplitude and phase relation with respect to the exciting force. This relationship can be challenging to determine when multiple modes are being used for conversion. Moreover, when motions are large enough (as expected with control), modes such as surge, pitch, and heave become nonlinearly coupled. This nonlinearly coupled WEC dynamic system hinders the use of the linear control design methods. Reference [29] presents an approximate approach for handling such nonlinearities in WEC control design. This paper shows that control of a WEC with heave-pitch-surge coupling at the second order can be approached as control of a linear time-varying system. In this model the heave mode excites the pitch mode, which in turn is coupled with the surge mode. The heave mode however is uncoupled to second order. This paper presents a linear quadratic Gaussian optimal control based on this argument. The controller proposed in this paper predict the excitation force by the past and the current information. The wave estimation is required to propose the controller. Compare to the some conventional controllers which are non-causal (ex. Complex Conjugate Control [21]), the presenting controller is causal. This control aims at maximizing the energy harvested over a receding time horizon. The excitation forces in the 3-DoF are estimated using an extended Kalman filter. The optimal estimated states are used to compute the Time-Varying LQ optimal control of the WEC. Constraints on the WEC motion are accounted for in computing the control. The goal of this study is to demonstrate that, with proper design of the control, it is possible to exploit this nonlinear coupling between the modes so as to harvest more energy.

II. Problem set-up

A. Wave model

In this paper, the Bretschneider spectrum [30], [31] is used. This spectrum has the form:

$$S(\omega) = \frac{5}{16}\frac{\omega_p^4}{\omega^5}H_s^2 e^{-5\omega_p^4/(4\omega^4)} \quad (1)$$

Where ω_p is the peak frequency of a given wave, and H_s is the significant height of the wave.

B. Dynamic Model

The dimensions of the buoy used in this paper are shown in Fig. 1. The presenting buoy has a mass of $858.4\ kg$, a volume of $0.8578\ m^3$ and a diagonal inertia matrix of $[83.932\,, 83.932\,, 137.5252]\ kg.m^2$. The total height of the buoy is $0.7294\ m$ while the height of the cylindrical part is $0.38\ m$ which has a radius of $0.8604\ m$. The Mean Water Level is defined at $z = 0\ m$.

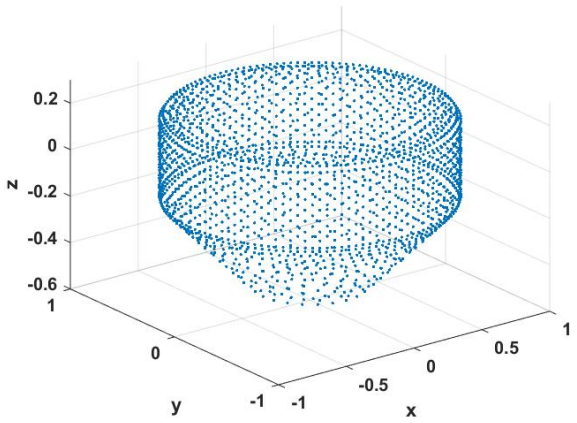

Fig. 1: The dimensions of the buoy

Since the conical part of the buoy will make the dynamics more complex, in deriving the equation of motion, a cylindrical shape is assumed. Additionally, to keep the assumption valid, the motion of the buoy will be constrained to remain in the cylindrical part. In other words, the conical part of the buoy will be always fully submerge in the water. Fig. 2 shows a side view of the buoy. In the figure, d_1, d_3 and θ_5 represents the surge, heave, and pitch motion respectively. The radius of the buoy is denoted as R, the mass of the buoy is denoted as m. h denotes the height between the center of gravity and the bottom of the buoy. The two nodes G and B denote the center of gravity and center of buoyancy respectively. For the sake of demonstrating the derivation of the dynamics, the buoy shown in the figure is not at the equilibrium point. The buoy is at some moment with certain surge, heave and pitch motion. Hence, in the figure, the center of gravity is not co-located with the center of buoyancy. In this paper, the assumption made is the three-degree-of-freedom motion can be controlled directly. Since this paper focus on presenting the optimal control theory, the development of the Power take-off system is beyond the scope of this paper.

The heave motion is uncoupled from the surge and pitch motion [32]. So the heave motion can be expressed as blow (neglecting the high order terms):

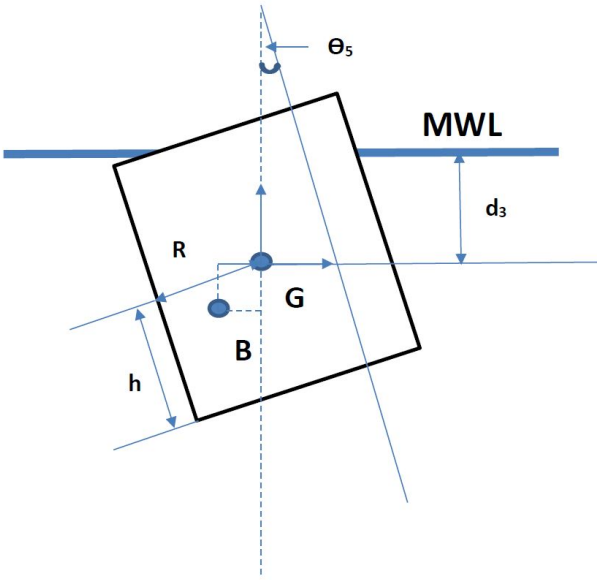

Fig. 2: Geometry of a 3-DoF cylindrical Buoy; MWL is the mean water level

$$\begin{aligned}\left(m + m_\infty^{33}\right)\ddot{d}_3 + b_3\dot{d}_3 + K_3 d_3 \\ = F_e^3 + F_{rad}^3 + u_3\end{aligned} \quad (2)$$

where $K_3 = \rho g \pi R^2$ and m is the mass of the rigid body, m_∞^{33} represents the added mass of heave mode. The total mass which is the summation of m and m_∞^{33} can be denoted as M^3. b_3 is the coefficient of viscous damping. F_e^3, F_{rad}^3 and u_3 represents the excitation force, radiation force and control force in heave mode. While the surge and pitch motion can be expressed in matrix format:

$$[M]\ddot{\vec{x}} + [C]\dot{\vec{x}} + [K]\vec{x} = \vec{F}_e + \vec{F}_{rad} + \vec{u} \quad (3)$$

where the excitation force vector is $\vec{F}_e = [F_e^1\,, F_e^5]^T$, the control force vector is $\vec{u} = [u_1\,, u_5]^T$ which is also the Power take-off (PTO) force. The radiation damping force vector is $\vec{F}_{rad} = [F_{rad}^1\,, F_{rad}^5]^T$. The radiation damping force can be approximated by a state space model instead of using convolution integral [33].

$$\begin{aligned}\dot{\vec{x}}_r &= A_r\vec{x}_r + B_r\dot{\vec{x}} \\ \vec{F}_{rad} &= C_r\vec{x}_r\end{aligned}$$

Where A_r, B_r, C_r matrices can be computed from the radiation impulse response function.

In Eq.(3) the matrix $[M]$ is:

$$[M] = \begin{bmatrix} m + m_\infty^{11} & m_\infty^{15} \\ I_\infty^{51} & I_5 + I_\infty^{55} \end{bmatrix},$$

the matrix $[C]$ is:

$$[C] = \begin{bmatrix} b_1 & 0 \\ 0 & b_5 \end{bmatrix},$$

and the matrix $[K]$ is:

$$[K] = \begin{bmatrix} K_{moor} & 0 \\ 0 & K_{55} \end{bmatrix},$$

where K_{moor} is the mooring stiffness in surge direction. K_{55} is the pitch restoring coefficient which has a constant part and a time-varying part. So we can express K_{55} as:

$$K_{55} = K_c + K_p(t) \tag{4}$$

where the constant part $K_c = \frac{\pi\rho g R^2}{4}\left(R^2 + 2h^2\right)$ and the time-varying part $K_p(t) = \pi\rho g R^2 h d_3$. So in the equation of motion of surge and pitch, the heave motion influence the time varying stiffness. This phenomenon is known as parametric excitation [34]. All the coefficients of hydrodynamics and hydrostatics are computed from the open source software NEMOH [35] which implements a boundary element method.

C. Wave forecasting

To implement the LQG controller we need to predict the excitation force. The wave excitation force can be approximated by Fourier Series:

$$\hat{F}_e = \sum_{i=1}^{n} (A_i \cos(\omega_i t) + B_i \sin(\omega_i t)) \tag{5}$$

where n represents the number of Fourier terms used to approximate the excitation force. Since in our problem the surge and pitch motion is excited by heave motion, two Kalman filters are built to estimate the states: one for the coupled motion (surge and pitch), and one for the heave motion. Although we can combine those two Kalman filters into one, separating them reduces the computational cost. They are still coupled because the heave motion excites the surge and pitch motion. So the current estimation of heave displacement will be fed into a Kalman filter to estimate the states of surge and pitch. In Fig. 3, the Kalman Filter

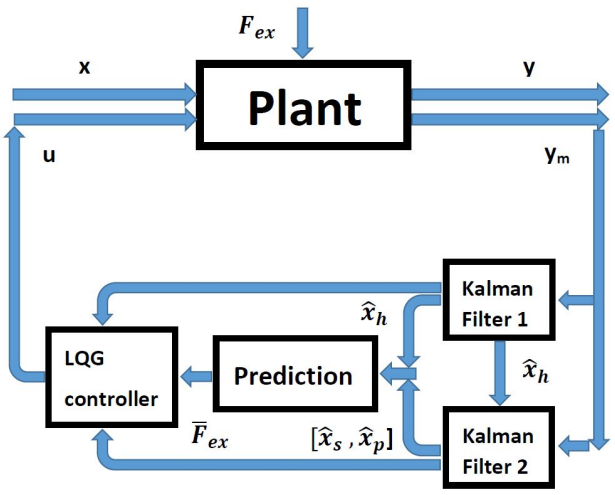

Fig. 3: The flow chart of LQG optimal controller

1 estimates the states of heave motion. The state vector for Kalman Filter 1 is $\hat{\mathbf{x}}^h = [d_3, \dot{d}_3, \vec{x}_r^3, \vec{A}^3, \vec{B}^3, \vec{w}^3]^T$. The states estimated by Kalman Filter 2 are $\hat{\mathbf{x}}^c = [d_1, \theta_5, \dot{d}_1, \dot{\theta}_5, \vec{x}_r^c, \vec{A}^1, \vec{B}^1, \vec{A}^5, \vec{B}^5, \vec{w}^1, \vec{w}^5]^T$, where $\vec{A}^j$, $\vec{B}^j$, and $\vec{w}^j$ represent the coefficients and frequencies of cosine and sine functions, respectively, in the excitation force Fourier expansion. The superscript of those parameters j can be 1, 3 and 5 which denotes the surge, heave and pitch motion respectively. The subscript h denotes the states of the heave motion, c denotes the states of the coupled motion.

The equations of motion of the dynamic system described in Eq. (3) and Eq. (2) can be written as a state space model. Let the first part of the states of Kalman Filter 1 be $\mathbf{x}_h = [d_3, \dot{d}_3, \vec{x}_r^3]^T$. Also define $\mathbf{x}^c = [d_1, \theta_5, \dot{d}_1, \dot{\theta}_5, \vec{x}_r^c]^T$. Hence the equations of motion can be written as:

$$\dot{\mathbf{x}}^h(t) = F^3(t)\mathbf{x}^h(t) + G^3(t)u_3(t) + c^3(t) \tag{6}$$

$$\dot{\mathbf{x}}^c(t) = F^c(t)\mathbf{x}^c(t) + G^c(t)\mathbf{u}^c(t) + c^c(t) \tag{7}$$

where

$$F^3(t) = \begin{bmatrix} 0 & 1 & \mathbf{0} \\ -\frac{1}{M^3}K_3 & -\frac{1}{M^3}b_3 & -\frac{1}{M^3}C_r^3 \\ \mathbf{0} & B_r^3 & A_r^3 \end{bmatrix} \tag{8}$$

$$G^3 = \begin{bmatrix} 0 \\ \frac{1}{M^3} \\ \mathbf{0} \end{bmatrix} \tag{9}$$

$$c^3(t) = \begin{bmatrix} 0 \\ \frac{1}{M^3} \\ \mathbf{0} \end{bmatrix} \hat{F}_e^3 \tag{10}$$

and,

$$F^c(t) = \begin{bmatrix} \begin{bmatrix} 0 & 0 \\ 0 & 0 \end{bmatrix} & \begin{bmatrix} 1 & 0 \\ 0 & 1 \end{bmatrix} & \begin{bmatrix} \mathbf{0} \\ \mathbf{0} \end{bmatrix} \\ -[M]^{-1}[K] & -[M]^{-1}[C] & -[M]^{-1}C_r \\ \begin{bmatrix} \mathbf{0} & \mathbf{0} \end{bmatrix} & B_r & A_r \end{bmatrix} \tag{11}$$

$$G^c = \begin{bmatrix} \begin{bmatrix} 0 & 0 \\ 0 & 0 \end{bmatrix} \\ [M]^{-1} \\ \begin{bmatrix} \mathbf{0} & \mathbf{0} \end{bmatrix} \end{bmatrix} \tag{12}$$

$$c^c(t) = \begin{bmatrix} \begin{bmatrix} 0 & 0 \\ 0 & 0 \end{bmatrix} \\ [M]^{-1} \\ \begin{bmatrix} \mathbf{0} & \mathbf{0} \end{bmatrix} \end{bmatrix} \begin{bmatrix} \hat{F}_e^1 \\ \hat{F}_e^5 \end{bmatrix} \tag{13}$$

The $\hat{F}_e$ represents the estimation of excitation force. In this paper, a short-term prediction for excitation force will be needed to compute the control. The sea states are assumed to be steady within this short period. Hence, the dynamics of the states for estimating the excitation force are:

$$\dot{\vec{A}} = \mathbf{0} \tag{14}$$

$$\dot{\vec{B}} = \mathbf{0} \tag{15}$$

$$\dot{\vec{w}} = \mathbf{0} \tag{16}$$

where $\vec{A} = [\vec{A}^1, \vec{A}^3, \vec{A}^5]^T$, $\vec{B} = [\vec{B}^1, \vec{B}^3, \vec{B}^5]^T$, $\vec{w} = [\vec{w}^1, \vec{w}^3, \vec{w}^5]^T$.

D. The Jacobian Matrices

To implement the Extended Kalman Filter, we need to construct the Jacobian matrices from the nonlinear system. The partial derivatives are computed for Eq. (6), Eq. (7) and Eqs. (14) to (16). To write the partial derivatives in matrix format, the matrices are defined:

$$\phi^c = \begin{bmatrix} \phi_c^1 & \phi_s^1 & \mathbf{0} & \mathbf{0} \\ \mathbf{0} & \mathbf{0} & \phi_c^5 & \phi_s^5 \end{bmatrix} \tag{17}$$

$$\phi^h = \begin{bmatrix} \phi_c^3 & \phi_s^3 \end{bmatrix} \tag{18}$$

$$D_\phi^c = \begin{bmatrix} D^1 & \mathbf{0} \\ \mathbf{0} & D^5 \end{bmatrix} \tag{19}$$

$$D_\phi^h = D^3 \tag{20}$$

where

$$\begin{aligned} \phi_c^j &= \left[\cos(\omega_1^j t) ... \cos(\omega_n^j t)\right] \\ \phi_s^j &= \left[\sin(\omega_1^j t) ... \sin(\omega_n^j t)\right] \\ j &= 1,\, 3,\, 5 \end{aligned} \tag{21}$$

where D^1, D^3 and D^5 are row vectors which contains n elements. The k^{th} component of D^j vectors can be expressed as:

$$\begin{aligned} D_k^j = -A_k^j \sin(\omega_k^j t)t + B_k^j \cos(\omega_k^j t)t \\ j = 1,\, 3,\, 5 \\ k = 1, ..., n \end{aligned} \tag{22}$$

$$\mathscr{F}^c(t) = \begin{bmatrix} F^c(t) & \begin{bmatrix} \mathbf{0} & \mathbf{0} & \mathbf{0} & \mathbf{0} & \mathbf{0} & \mathbf{0} \\ & [M]^{-1}\phi^c & & & [M]^{-1}D_\phi^c & \\ \mathbf{0} & \mathbf{0} & \mathbf{0} & \mathbf{0} & \mathbf{0} & \mathbf{0} \end{bmatrix} \\ \mathbf{0} & \mathbf{0} \\ \vdots & \\ \mathbf{0} & \mathbf{0} \end{bmatrix} \tag{23}$$

In this paper, it is assumed that the displacement and velocity will be measured for each of the surge, pitch and heave motions. For the coupled motion we have:

$$y_m^c = \left[d_1,\, \theta_5,\, \dot{d}_1,\, \dot{\theta}_5\right] + v^c(t) \tag{24}$$

where $v^c(t) \sim N(\mathbf{0}, Q^c(t))$ which is assumed to be white noise with normal distribution. So the Jacobian matrix of the output model of surge and pitch motion is:

$$\mathscr{H}^c(t) = \begin{bmatrix} 1 & 0 & 0 & 0 & \mathbf{0} \\ 0 & 1 & 0 & 0 & \mathbf{0} \\ 0 & 0 & 1 & 0 & \mathbf{0} \\ 0 & 0 & 0 & 1 & \mathbf{0} \end{bmatrix} \tag{25}$$

Similarly, the Jacobian matrices of Heave motion can be derived:

$$\mathscr{F}^h(t) = \begin{bmatrix} F^h(t) & \begin{bmatrix} \mathbf{0} & \mathbf{0} & \mathbf{0} \\ & \frac{1}{M^3}\phi^h & \frac{1}{M^3}D_\phi^h \\ \mathbf{0} & \mathbf{0} & \mathbf{0} \end{bmatrix} \\ \mathbf{0} & \mathbf{0} \\ \vdots & \\ \mathbf{0} & \mathbf{0} \end{bmatrix} \tag{26}$$

$$\mathscr{H}^h(t) = \begin{bmatrix} 1 & 0 & 0 & 0 & \mathbf{0} \\ 0 & 1 & 0 & 0 & \mathbf{0} \end{bmatrix} \tag{27}$$

The output model of heave is:

$$y_m^h = \left[d_3,\, \dot{d}_3\right] + v^h(t) \tag{28}$$

where $v^h(t) \sim N(\mathbf{0}, Q^h(t))$ is the measurement noise of heave motion which is also assumed to be white noise.

III. Time-varying LQG Control

The optimal control problem is split into two parts. The first part is the LQ optimal controller which computes the control assuming the availability of the estimated states; this parts requires, as input, the wave prediction and the estimation of the states. The second part is a LQ optimal estimator which generates the estimation and prediction.

A. The LQ control law

The energy captured by the WEC is defined as:

$$E = \int_0^{T_{end}} (u_1(t)\dot{d}_1 + u_3(t)\dot{d}_3 + u_5(t)\dot{\theta}_5)dt \tag{29}$$

So we can define the Lagrangian for surge and pitch motion as:

$$L^c = (\mathbf{u}^c)^T W^c \mathbf{x}^c + \frac{1}{2}(\mathbf{u}^c)^T R^c \mathbf{u}^c \tag{30}$$

where the matrices W and R are selected as:

$$W^c = \begin{bmatrix} 0 & 0 \\ 0 & 0 \\ 1 & 0 \\ 0 & 1 \\ \mathbf{0} & \mathbf{0} \end{bmatrix} \tag{31}$$

$$R^c = \begin{bmatrix} \epsilon_1 & 0 \\ 0 & \epsilon_5 \end{bmatrix} \tag{32}$$

The Lagrangian can be written in the following convex format:

$$\begin{aligned} L^c = \frac{1}{2}(\mathbf{x}^c)^T (Q^c - W^c (R^c)^{-1} (W^c)^T)\mathbf{x}^c + \\ \frac{1}{2}(\mathbf{u}^c + (R^c)^{-1}(W^c)^T \mathbf{x}^c)^T R^c (\mathbf{u}^c + (R^c)^{-1}(W^c)^T \mathbf{x}^c) \end{aligned} \tag{33}$$

If we do not included any constraint for the states of surge and pitch, the state penalty matrix is set as $Q^c = [\mathbf{0}]$. Let

us define $A_1^c = (Q^c - W^c(R^c)^{-1}(W^c)^T)$, $B_1^c = R^c$ and $\mathbf{U}_1^c = (\mathbf{u}^c + (R^c)^{-1}(W^c)^T\mathbf{x}^c)$. The dynamics can also be written as:

$$\dot{\mathbf{x}^c}(t) = F_1^c(t)\mathbf{x}^c(t) + G^c(t)\mathbf{U}_1^c(t) + c^c(t) \tag{34}$$

where $F_1^c = F^c(t) - G^c(R^c)^{-1}(W^c)^T$. The Riccati equation and its auxiliary equation can be solved as:

$$\dot{S}^c + S^cF_1^c(t) + F_1^c(t)^TS^c - S^cG^c(B_1^c)^{-1}(G^c)^TS^c + A_1^c = \vec{0} \tag{35}$$

$$\dot{k}^c + F_1^c(t)^Tk^c - S^cG^c(B_1^c)^{-1}(G^c)^Tk^c + S^cc^c(t) = \vec{0} \tag{36}$$

Since there is no constraint on the final conditions, then the final conditions of the Riccati and Auxiliary equations are $S^c(t_f) = \vec{0}$, $k^c(t_f) = \vec{0}$. These two equations can be propagated backward to get the time history of the optimal feedback gain. The optimal control law is:

$$\mathbf{U}_1^{c*} = -(B_1^c)^{-1}(G^c)^T\lambda^c \tag{37}$$

Finally the expression of the control force can be obtained after transforming back $\mathbf{U}_1^{c*}$ to get:

$$\begin{aligned}\mathbf{u}^{c*} = -((B_1^c)^{-1}(G^c)^TS^c(t) + \\ (B_1^c)^{-1}(W^c)^T)\mathbf{x}^c(t) - (B_1^c)^{-1}(G^c)^Tk^c(t)\end{aligned} \tag{38}$$

A similar approach can be developed for the heave control to get:

$$\begin{aligned}\mathbf{u}^{h^*} = -((B_1^h)^{-1}(G^h)^TS^h(t) + \\ (B_1^h)^{-1}(W^h)^T)\mathbf{x}^h(t) - (B_1^h)^{-1}(G^h)^Tk^h(t)\end{aligned} \tag{39}$$

where

$$W^c = \begin{bmatrix}0\\1\\\mathbf{0}\end{bmatrix} \tag{40}$$

$$B_1^h = R^c = \epsilon_3 \tag{41}$$

B. The LQ optimal estimator

As indicated in Fig. 3, two Kalman Filters are implemented to generate estimation. The procedure of updating the estimation is introduced here.

1. Initialization:

$$\hat{\mathbf{x}}(t_0) = \hat{\mathbf{x}}_0 \tag{42}$$

$$P_0 = E(\tilde{\mathbf{x}}(t_0)\tilde{\mathbf{x}}(t_0)^T) \tag{43}$$

2. Compute Current Kalman Gain based on current estimation:

$$K_k = P_k^-\mathscr{H}_k^T(\hat{\mathbf{x}}_k^-)(\mathscr{H}_k(\hat{\mathbf{x}}_k^-)P_k^-\mathscr{H}_k^T(\hat{\mathbf{x}}_k^-) + R_k)^{-1} \tag{44}$$

3. Update the estimation:

$$\begin{aligned}\hat{\mathbf{x}}_k^+ &= \hat{\mathbf{x}}_k^- + K_k(\tilde{y}_k - h(\hat{\mathbf{x}}_k^-)) \\ P_k^+ &= (I - K_k\mathscr{H}_k(\hat{\mathbf{x}}_k^-))P_k^-\end{aligned} \tag{45}$$

The propagation of the state error covariance matrix can be carried out using the equation:

$$\dot{P}(t) = \mathscr{F}(t)P(t) + P(t)\mathscr{F}^T(t) + \mathscr{G}(t)Q(t)\mathscr{G}^T(t) \tag{46}$$

Once the estimation of the states at a current time is available, Eq. (5) can be used for predicting the excitation force for a future short period.

IV. Simulation Results

A Bretschneider spectrum wave is assumed in all the simulations, with a significant height of $0.5\ m$ and a peak period of $1.5708\ s$. The wave is generated using contains 1260 frequencies ranging from 0.01 to 12.6. The control update rate in the simulation is set to be $50\ Hz$. The details for the performance of LQG controller will be presented in Section. IV-B, while the method to compute the initial guess will be addressed in Section. IV-A. The Capture Width Ratio (CWR) is the criteria used for assessing the performance. The CWR can be computed by [36]:

The buoy described in Section. II is used in the simulation.

$$CWR = \frac{p_m}{Dp_w} \tag{47}$$

where p_m is the mean absorbed power, D is the characteristic dimension of the buoy which is selected to be the diameter of the cylindrical part of the buoy, and p_w is the energy transport which can be computed as [37]:

$$p_w = \frac{1}{2}\rho g^2\int_0^\infty \frac{S(\omega)}{\omega}d\omega \tag{48}$$

Additionally, the key parameters for the simulation are summarized in Table. I.

TABLE I: Summarize of the key parameters for the simulation

$m\ (kg)$	858.4
$I_5\ (kg.m^2)$	83.932
$h\ (m)$	0.3647
$R\ (m)$	0.8604
$K_{moor}\ (N/m)$	126.6462
$b_1\ (N.s/m)$	156.4364
$b_3\ (N.s/m)$	253.9528
$b_5\ (N.m.s)$	37.0737
ϵ_1	5×10^{-6}
ϵ_3	5×10^{-6}
ϵ_5	8×10^{-5}

A. Initialization

The estimation algorithm described in Section. III-B uses on a finite number of frequencies to construct the Fourier Series expansion of the excitation force. Because of the computational cost, a few number frequencies is used in the estimator. A Least Square (LS) method is used here to initialize each of the $\vec{A}$, $\vec{B}$ and $\vec{\omega}$ vectors. Let the fundamental frequency be $w_0 = \frac{2\pi}{T_w}$, where T_w is the size of the window for initialization. Eq. (17) and Eq. (18) are the basis functions which will be used in the LS method where $w_k^j = kw_0^j$. The k represents the

number of cosine and sine functions in the estimator. There are two parameters to be selected, one is the number of frequencies k, and the other is the size of the LS window T_w. Fig. 4 is used to demonstrate the impact of k on the computational cost and energy absorption. The corresponding operating time of the WEC is 30 s. Based on Fig. 4, $k = 18$ is selected for all the numerical tests which requires 0.0958 s to compute each control.

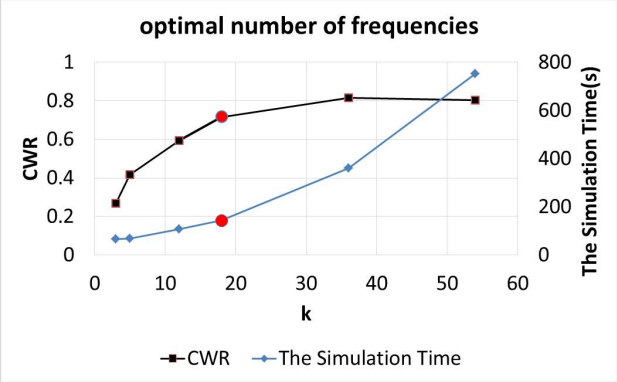

Fig. 4: The computational cost of simulation and the energy absorption from different number of frequencies

The window size T_w also needs to be selected to get a good initial guess. Fig. 5 shows the energy absorption for different sizes of the window when $k = 18$. From Fig. 5, $T_w = 25$ s is selected.

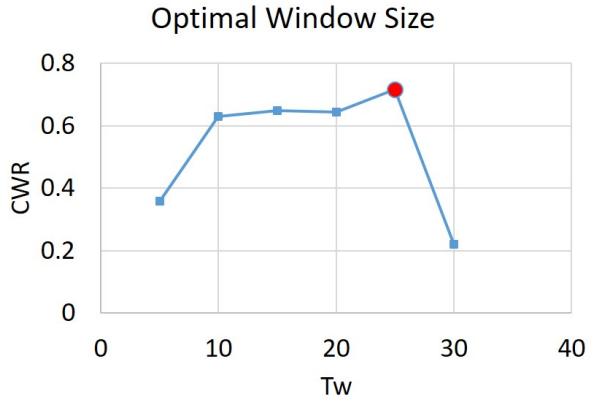

Fig. 5: The energy absorption from different size of window

B. The performance of LQG controller

In this section, the performance of LQG controller will be presented. The total simulation time extends to 200 s. The motion is constrained; the constraint for the surge is 1 m, and for the pitch is 1 rad. Since the Mean Water Level is defined at $z = 0$ m, to keep the conical part of the buoy always be submerge in the water and to constrain the buoy floating on the water without fully sinking, the maximum heave motion is constrained to be 0.2 m. Fig. 6 shows the wave elevation at different frequencies of Bretschneider wave. The absorbed energy is shown in Figs. 7– 9. Fig. 7 compares between the energy absorption using LQG controller and energy absorption using LQ controller. The latter represents the ideal situation when we assume we have perfect knowledge of the wave. The energy captured by LQG controller is around 61.6% of the energy captured by LQ controller. In Fig. 8 made the comparison between the energy captured by the system with parametric excitation model and the system with a linear model that does not account for parametric excitation. The system without parametric excitation means the heave motion does not excite the surge and pitch motions. In Fig. 8 the total energy captured by the system with parametric excitation is 3.2×10^4 J compared to 2.899×10^4 J that is the energy captured by the system without parametric excitation. In Fig. 9, the energy captured by surge, heave, and pitch are 1.101×10^4 J, 0.899×10^4 J and 1.199×10^4 J respectively. So the total energy is 3.56 times the energy captured by heave motion only. Note that it can be shown that the maximum ratio between the total energy and heave energy is 3 when the system is linear and in the absence of viscous damping.

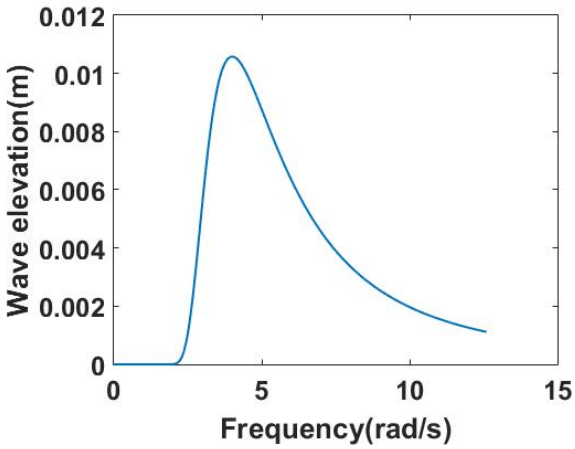

Fig. 6: The wave elevation

C. The test of different sea states

To validate the performance of the LQG controller, the controller is tested with different sea states. Those different sea states have the same significant height of 0.5 m, but different peak period which varies from 6 s to 12 s. Fig. 10 shows the power extraction decreases from 108.18 W to 30.71 W when the peak period of the wave increases. Detailedly, the CWR of the case when the buoy interacts with the wave has a peak period of 7 s is 0.0665. Compared to the CWR of the wave which has a small peak period, the CWR presented in this section is significantly lower. For a long peak period wave, the energy contains in the wave increase significantly. To absorb the energy in the wave, a larger motion of the buoy is required. Moreover, based on the proposed shape, most of the energy contains in the heave mode when the peak period is high. However, the heave is substantially constrained to keep

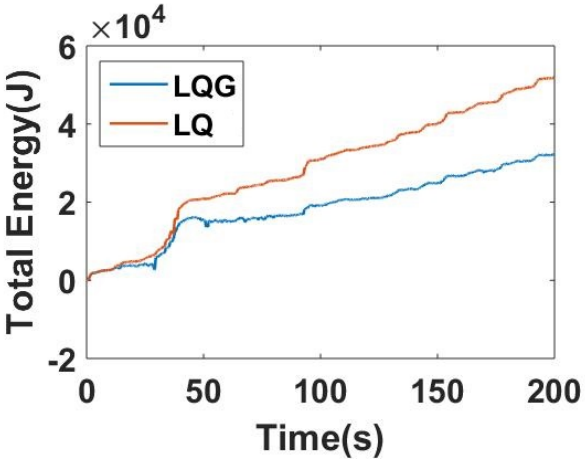

Fig. 7: The total extracted energy

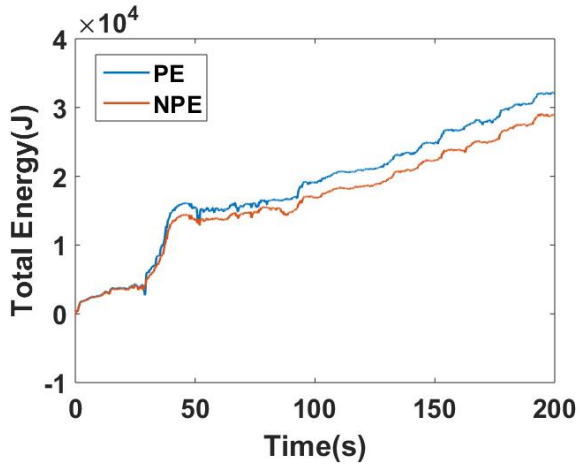

Fig. 8: The total extracted energy

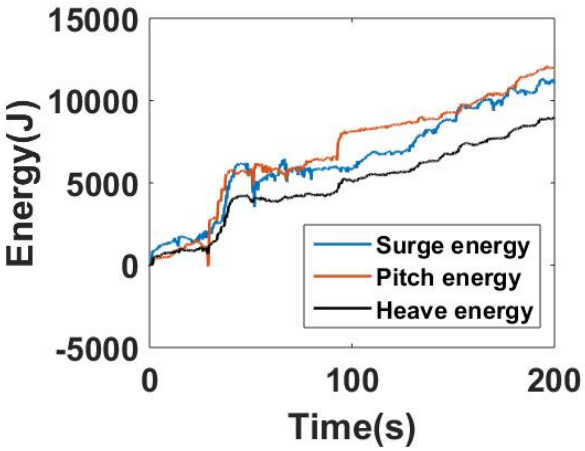

Fig. 9: The energy extracted from surge, heave and pitch motion

the motion feasible. Consequently, the energy extracted from a long peak period wave is small due to the constraint. Since the energy contains in the wave is more, but the absorbed energy is less, the CWR is much lower than the CWR for a low peak period wave. Additionally, the energy extracted from three modes when the peak period of the wave is 7 s decreases 2.05 times the energy extracted from heave-only mode. As we mentioned in this section, most of the energy contains in the heave mode when the peak period is high. So the energy ratio between three modes and heave only mode decreases.

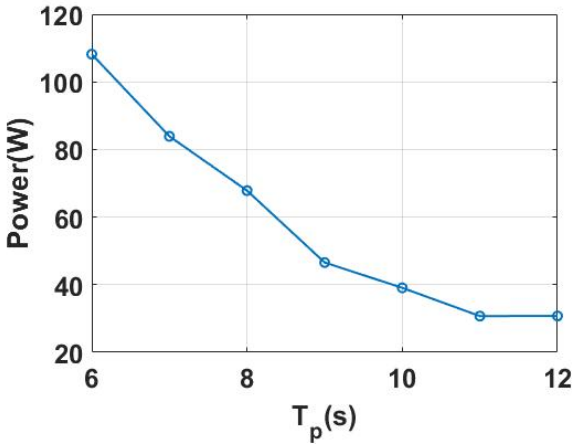

Fig. 10: The average power extraction under different sea states

ACKNOWLEDGEMENT

This material is based upon work supported by the National Science Foundation under Grant Number 1635362

CONCLUSION

For a three-degree-of-freedom (3-Dof) WEC, a time-varying Linear Quadratic Gaussian (LQG) controller is developed. For the control purpose, a prediction for the excitation force is made based on the estimation of its parameters in Fourier Series expansion. The controller is tested with a small point absorber with the surge, heave and pitch motion. The key findings of this paper are: first, a WEC with 3-Dof actuation capability can extract more energy than three folds of the energy extracted from heave motion only. Second, the energy extracted from the system with parametric excitation is more than that extracted with a model that does not account for parametric excitation. Finally, the previous conclusions are still valid when we have only estimates of the excitation force.

REFERENCES

[1] A. Clément, P. McCullen, A. Falcão, A. Fiorentino, F. Gardner, K. Hammarlund, G. Lemonis, T. Lewis, K. Nielsen, S. Petroncini *et al.*, "Wave energy in europe: current status and perspectives," *Renewable and sustainable energy reviews*, vol. 6, no. 5, pp. 405–431, 2002.

[2] R. Bedard, M. Previsic, G. Hagerman, B. Polagye, W. Musial, J. Klure, A. von Jouanne, U. Mathur, J. Partin, C. Collar *et al.*, "North american ocean energy statusmarch 2007," in *7th European Wave and Tidal Energy Conference (EWTEC), Porto, Portugal, September*. Citeseer, 2007, pp. 11–13.

[3] M. Leijon, C. Boström, O. Danielsson, S. Gustafsson, K. Haikonen, O. Langhamer, E. Strömstedt, M. Stålberg, J. Sundberg, O. Svensson *et al.*, "Wave energy from the north sea: Experiences from the lysekil research site," *Surveys in geophysics*, vol. 29, no. 3, pp. 221–240, 2008.

[4] B. Liang, Z. Shao, G. Wu, M. Shao, and J. Sun, "New equations of wave energy assessment accounting for the water depth," *Applied Energy*, vol. 188, pp. 130 – 139, 2017. [Online]. Available: http://www.sciencedirect.com/science/article/pii/S0306261916317585

[5] B. Reguero, I. Losada, and F. Mndez, "A global wave power resource and its seasonal, interannual and long-term variability," *Applied Energy*, vol. 148, pp. 366 – 380, 2015. [Online]. Available: http://www.sciencedirect.com/science/article/pii/S030626191500416X

[6] R. Coe, G. Bacelli, D. Patterson, and D. Wilson, "Advanced wec dynamics & controls FY16 testing report," Sandia National Laboratories, Albuquerque, NM, Tech. Rep. SAND2016-10094, 2016.

[7] J.-B. Saulnier, T. Soulard, Y. Perignon, I. Le Crom, and A. Babarit, "About the use of 3 rd-generation wave prediction models for estimating the performance of wave energy converters in coastal regions," in *EWTEC*, 2013.

[8] E. Rusu and F. Onea, "Estimation of the wave energy conversion efficiency in the atlantic ocean close to the european islands," *Renewable Energy*, vol. 85, pp. 687–703, 2016.

[9] I. López, B. Pereiras, F. Castro, and G. Iglesias, "Performance of owc wave energy converters: influence of turbine damping and tidal variability," *International Journal of Energy Research*, vol. 39, no. 4, pp. 472–483, 2015.

[10] A. Sproul and N. Weise, "Analysis of a wave front parallel wec prototype," *IEEE Transactions on Sustainable Energy*, vol. 6, no. 4, pp. 1183–1189, 2015.

[11] F. He, Z. Huang, and A. W.-K. Law, "An experimental study of a floating breakwater with asymmetric pneumatic chambers for wave energy extraction," *Applied Energy*, vol. 106, pp. 222 – 231, 2013. [Online]. Available: http://www.sciencedirect.com/science/article/pii/S0306261913000226

[12] M. Durand, A. Babarit, B. Pettinotti, O. Quillard, J. Toularastel, and A. Clément, "Experimental validation of the performances of the searev wave energy converter with real time latching control," *EWTEC, Porto*, 2007.

[13] J. Cordonnier, F. Gorintin, A. De Cagny, A. Clément, and A. Babarit, "Searev: Case study of the development of a wave energy converter," *Renewable Energy*, vol. 80, pp. 40–52, 2015.

[14] S. Astariz and G. Iglesias, "The economics of wave energy: A review," *Renewable and Sustainable Energy Reviews*, vol. 45, pp. 397–408, 2015.

[15] J. P. Kofoed, P. Frigaard, E. Friis-Madsen, and H. C. Sørensen, "Prototype testing of the wave energy converter wave dragon," *Renewable energy*, vol. 31, no. 2, pp. 181–189, 2006.

[16] J. Fernández Chozas, "Una aproximación al aprovechamiento de la energía de las olas para generación de electricidad," *Proyecto Fin de Carrera. UPM*, 2008.

[17] A. Weinstein, G. Fredrikson, M. Parks, and K. Nielsen, "Aquabuoy-the offshore wave energy converter numerical modeling and optimization," in *OCEANS'04. MTTS/IEEE TECHNO-OCEAN'04*, vol. 4. IEEE, 2004, pp. 1854–1859.

[18] C. C. Mei, "Power extraction from water waves," *Journal of Ship Research*, vol. 20, pp. 63–66, June 1976.

[19] J.N.Newman, "The interaction of stationary vessels with regular waves," in *Proceeding 11th symposium, Naval hydrodynamics*, London, 1976. [Online]. Available: http://journals.cambridge.org/article_S0022112076001109

[20] D. V. Evans, "A theory for wave-power absorption by oscillating bodies," *Journal of Fluid Mechanics*, vol. 77, pp. 1–25, 9 1976. [Online]. Available: http://journals.cambridge.org/article_S0022112076001109

[21] J. Falnes, *Ocean waves and oscillating systems: linear interactions including wave-energy extraction*. Cambridge university press, 2002.

[22] W. Cummins, D. T. M. B. W. D. C., and D. W. T. M. Basin, *The Impulse Response Function and Ship Motions*, ser. Report (David W. Taylor Model Basin). Navy Department, David Taylor Model Basin, 1962. [Online]. Available: https://books.google.com/books?id=GLLANwAACAAJ

[23] J. Falnes, "A review of wave-energy extraction," *Marine Structures*, vol. 20, no. 4, pp. 185–201, 2007.

[24] U. A. Korde, "On control approaches for efficient primary energy conversion in irregular waves," in *OCEANS '98 Conference Proceedings*, vol. 3, Sep 1998, pp. 1427–1431 vol.3.

[25] F. Fusco and J. V. Ringwood, "Hierarchical robust control of oscillating wave energy converters with uncertain dynamics," *IEEE Transactions on Sustainable Energy*, vol. 5, no. 3, pp. 958–966, July 2014.

[26] J. Ringwood, G. Bacelli, and F. Fusco, "Energy-maximizing control of wave-energy converters: The development of control system technology to optimize their operation," *Control Systems, IEEE*, vol. 34, no. 5, pp. 30–55, Oct 2014.

[27] G. Bacelli and J. V. Ringwood, "Numerical optimal control of wave energy converters," *IEEE Transactions on Sustainable Energy*, vol. 6, no. 2, pp. 294–302, 2015.

[28] G. Li and M. R. Belmont, "Model predictive control of sea wave energy converters part i: A convex approach for the case of a single device," *Renewable Energy*, vol. 69, no. 0, pp. 453 – 463, 2014. [Online]. Available: http://www.sciencedirect.com/science/article/pii/S0960148114002456

[29] J. Scruggs, S. Lattanzio, A. Taflanidis, and I. Cassidy, "Optimal causal control of a wave energy converter in a random sea," *Applied Ocean Research*, vol. 42, pp. 1 – 15, 2013. [Online]. Available: http://www.sciencedirect.com/science/article/pii/S0141118713000205

[30] C. Bretschneider, "A one-dimensional gravity wave spectrum," *Ocean Wave Spectra*, pp. 41–65, 1963.

[31] M. Oosterveld, *Proceedings: 15th International Towing Tank Conference : ITTC'78, The Hague, September 1978*. Netherlands Ship Model Basin, 1978. [Online]. Available: https://books.google.com/books?id=RjnynQEACAAJ

[32] O. Abdelkhalik, S. Zou, R. Robinett, G. Bacelli, D. Wilson, and U. Korde, "Multi resonant feedback control of three-degree-of-freedom wave energy converters," *IEEE Transactions on Sustainable Energy*, 2016, in review.

[33] Z. Yu and J. Falnes, "State-space modelling of a vertical cylinder in heave," *Applied Ocean Research*, vol. 17, no. 5, pp. 265–275, 1995.

[34] A. Nayfeh and D. Mook, *Nonlinear Oscillations*, ser. Wiley Classics Library. Wiley, 2008. [Online]. Available: https://books.google.com/books?id=sj3ebg7jRaoC

[35] A. Babarit and G. Delhommeau, "Theoretical and numerical aspects of the open source bem solver nemoh," in *11th European Wave and Tidal Energy Conference (EWTEC2015)*, 2015.

[36] A. Babarit, "A database of capture width ratio of wave energy converters," *Renewable Energy*, vol. 80, pp. 610–628, 2015.

[37] Ø. Y. Rogne, "Numerical and experimental investigation of a hinged 5-body wave energy converter," Ph.D. dissertation, University of Science and Technology, 2014.